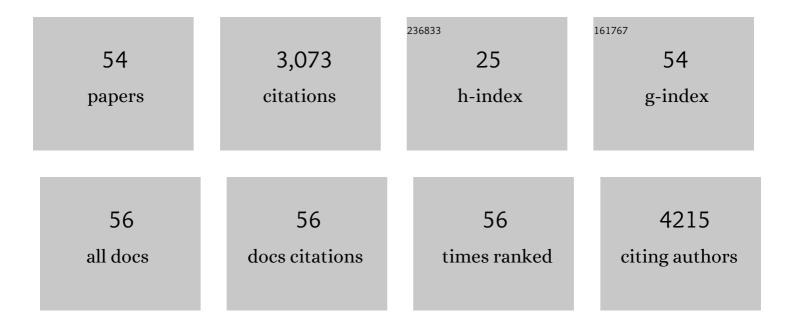
## Qiang-Qiang Meng

List of Publications by Year in descending order

Source: https://exaly.com/author-pdf/4911599/publications.pdf Version: 2024-02-01



#	Article	IF	CITATIONS
1	A flexible rechargeable aqueous zinc manganese-dioxide battery working at â^'20 °C. Energy and Environmental Science, 2019, 12, 706-715.	15.6	511
2	Co <sub>3</sub> O <sub>4</sub> Hexagonal Platelets with Controllable Facets Enabling Highly Efficient Visibleâ€Light Photocatalytic Reduction of CO <sub>2</sub> . Advanced Materials, 2016, 28, 6485-6490.	11.1	395
3	Toward Flexible Zincâ€Ion Hybrid Capacitors with Superhigh Energy Density and Ultralong Cycling Life: The Pivotal Role of ZnCl <sub>2</sub> Saltâ€Based Electrolytes. Angewandte Chemie - International Edition, 2021, 60, 990-997.	7.2	215
4	The S-functionalized Ti <sub>3</sub> C <sub>2</sub> Mxene as a high capacity electrode material for Na-ion batteries: a DFT study. Nanoscale, 2018, 10, 3385-3392.	2.8	139
5	Toward Flexible Zincâ€lon Hybrid Capacitors with Superhigh Energy Density and Ultralong Cycling Life: The Pivotal Role of ZnCl <sub>2</sub> Saltâ€Based Electrolytes. Angewandte Chemie, 2021, 133, 1003-1010.	1.6	130
6	Efficient photocatalytic H2 evolution, CO2 reduction and N2 fixation coupled with organic synthesis by cocatalyst and vacancies engineering. Applied Catalysis B: Environmental, 2021, 285, 119789.	10.8	120
7	Theoretical investigation of zirconium carbide MXenes as prospective high capacity anode materials for Na-ion batteries. Journal of Materials Chemistry A, 2018, 6, 13652-13660.	5.2	111
8	Make it stereoscopic: interfacial design for full-temperature adaptive flexible zinc–air batteries. Energy and Environmental Science, 2021, 14, 4926-4935.	15.6	108
9	Facet-dependent electrochemical properties of Co3O4 nanocrystals toward heavy metal ions. Scientific Reports, 2013, 3, 2886.	1.6	105
10	Lattice constant-dependent anchoring effect of MXenes for lithium–sulfur (Li–S) batteries: a DFT study. Nanoscale, 2019, 11, 8485-8493.	2.8	93
11	Role of the anatase/TiO <sub>2</sub> (B) heterointerface for ultrastable high-rate lithium and sodium energy storage performance. Nanoscale Horizons, 2020, 5, 150-162.	4.1	88
12	Toward efficient and high rate sodium-ion storage: A new insight from dopant-defect interplay in textured carbon anode materials. Energy Storage Materials, 2020, 28, 55-63.	9.5	85
13	Origin of High Photocatalytic Properties in the Mixed-Phase TiO <sub>2</sub> : A First-Principles Theoretical Study. ACS Applied Materials & Interfaces, 2014, 6, 12885-12892.	4.0	81
14	Infrared Response and Optoelectronic Memory Device Fabrication Based on Epitaxial VO <sub>2</sub> Film. ACS Applied Materials & Interfaces, 2016, 8, 32971-32977.	4.0	72
15	Freezeâ€Tolerant Hydrogel Electrolyte with High Strength for Stable Operation of Flexible Zincâ€lon Hybrid Supercapacitors. Small, 2022, 18, e2200055.	5.2	67
16	Theoretical prediction of MXene-like structured Ti <sub>3</sub> C <sub>4</sub> as a high capacity electrode material for Na ion batteries. Physical Chemistry Chemical Physics, 2017, 19, 29106-29113.	1.3	51
17	Tuning the indirect–direct band gap transition in the MoS <sub>2Ⲓx</sub> Se <sub>x</sub> armchair nanotube by diameter modulation. Physical Chemistry Chemical Physics, 2018, 20, 3608-3613.	1.3	51
18	In situ hydrogen from aqueous-methanol for nitroarene reduction and imine formation over an Au–Pd/Al2O3 catalyst. Chemical Communications, 2010, 46, 5918.	2.2	48

#	Article	IF	CITATIONS
19	Photocatalytic Performance of NiS/CdS Composite with Multistage Structure. ACS Applied Energy Materials, 2020, 3, 7736-7745.	2.5	48
20	Water splitting on TiO2 nanotube arrays. Catalysis Today, 2011, 165, 145-149.	2.2	47
21	Supramolecular Porous Network Formed by Molecular Recognition between Chemically Modified Nucleobases Guanine and Cytosine. Angewandte Chemie - International Edition, 2010, 49, 9373-9377.	7.2	45
22	Sub-20 nm-Fe <sub>3</sub> O <sub>4</sub> square and circular nanoplates: synthesis and facet-dependent magnetic and electrochemical properties. Chemical Communications, 2014, 50, 15952-15955.	2.2	36
23	Nanotoxicity of Boron Nitride Nanosheet to Bacterial Membranes. Langmuir, 2019, 35, 6179-6187.	1.6	36
24	Band structure engineering of anatase TiO2 by metal-assisted P-O coupling. Journal of Chemical Physics, 2014, 140, 174705.	1.2	29
25	Investigation of the facet-dependent performance of α-Fe <sub>2</sub> O <sub>3</sub> nanocrystals for heavy metal determination by stripping voltammetry. Chemical Communications, 2014, 50, 5011-5013.	2.2	28
26	A DFT Study of the Adhesion of Pd Clusters on ZnO SWNTs and Adsorption of Gas Molecules on Pd/ZnO SWNTs. Journal of Physical Chemistry C, 2009, 113, 21338-21341.	1.5	24
27	Revealing the role of oxygen vacancies on the phase transition of VO <sub>2</sub> film from the optical-constant measurements. RSC Advances, 2018, 8, 19151-19156.	1.7	23
28	One-Step Synthesis of a Nanosized Cubic Li <sub>2</sub> TiO <sub>3</sub> -Coated Br, C, and N Co-Doped Li <sub>4</sub> Ti <sub>5</sub> O <sub>12</sub> Anode Material for Stable High-Rate Lithium-Ion Batteries. ACS Applied Materials & Interfaces, 2019, 11, 25804-25816.	4.0	22
29	Charge driven lateral structural evolution of ions in electric double layer capacitors strongly correlates with differential capacitance. Physical Chemistry Chemical Physics, 2018, 20, 8054-8063.	1.3	20
30	Two-dimensional stable transition metal carbides (MnC and NbC) with prediction and novel functionalizations. Physical Chemistry Chemical Physics, 2018, 20, 25437-25445.	1.3	20
31	Nanotubes from Rutile TiO <sub>2</sub> (110) Sheets: Formation and Properties. Journal of Physical Chemistry C, 2010, 114, 9251-9256.	1.5	19
32	CO Oxidation by Lattice Oxygen on V <sub>2</sub> O <sub>5</sub> Nanotubes. Journal of Physical Chemistry C, 2011, 115, 14806-14811.	1.5	19
33	Homochiral Xanthine Quintet Networks Self-Assembled on Au(111) Surfaces. ACS Nano, 2011, 5, 6651-6660.	7.3	18
34	Electronic and optical properties of TiO2 nanotubes and arrays: a first-principles study. Physical Chemistry Chemical Physics, 2014, 16, 11519.	1.3	17
35	Enhanced reversible lithium storage for nano-Si with a <10â€ <sup>-</sup> nm homogenous porous carbon coating layer. Electrochimica Acta, 2018, 269, 1-10.	2.6	16
36	Modeling Interactions between Liposomes and Hydrophobic Nanosheets. Small, 2019, 15, e1804992.	5.2	16

QIANG-QIANG MENG

#	Article	IF	CITATIONS
37	Embedded iron nanoparticles by graphitized carbon as highly active yet stable catalyst for ammonia decomposition. Molecular Catalysis, 2017, 442, 147-153.	1.0	15
38	Synergy of a hierarchical porous morphology and anionic defects of nanosized Li4Ti5O12 toward a high-rate and large-capacity lithium-ion battery. Journal of Energy Chemistry, 2021, 54, 699-711.	7.1	13
39	Water oxidation on Nâ€Doped TiO <sub>2</sub> nanotube arrays. International Journal of Quantum Chemistry, 2012, 112, 2585-2590.	1.0	10
40	The graphene-supported non-noble metal catalysts activate ammonia decomposition: A DFT study. Chemical Physics, 2021, 548, 111249.	0.9	10
41	Well-Dispersed Monoclinic VO <sub>2</sub> Nanoclusters with Uniform Size for Sensitive near-Infrared Detection. ACS Applied Nano Materials, 2018, 1, 5044-5052.	2.4	9
42	The roles of surface oxygen vacancy over Mg4Ta2O9-x photocatalyst in enhancing visible-light photocatalytic hydrogen evolution performance. Catalysis Communications, 2018, 103, 29-33.	1.6	8
43	VC <sub>2</sub> and V <sub>1/2</sub> Mn <sub>1/2</sub> C <sub>2</sub> nanosheets with robust mechanical and thermal properties as promising materials for Li-ion batteries. Physical Chemistry Chemical Physics, 2019, 21, 1606-1613.	1.3	8
44	Impact of Oxygen Vacancy on Band Structure Engineering of n-p Codoped Anatase TiO2. Chinese Journal of Chemical Physics, 2015, 28, 155-160.	0.6	6
45	Alkyl Tail Aggregations Break Long-Range Ordering of Ionic Liquids Confined in Subnanometer Pores. Journal of Physical Chemistry C, 2018, 122, 27314-27322.	1.5	6
46	Lipid extraction by boron nitride nanosheets from liquid-ordered and liquid-disordered nanodomains. Nanoscale, 2018, 10, 14073-14081.	2.8	6
47	Electronic and optical properties of αâ€MoO <sub>3</sub> /TiO <sub>2</sub> heterostructures: A DFT study. International Journal of Quantum Chemistry, 2018, 118, e25681.	1.0	6
48	First-principles study on codoping effect to enhance photocatalytic activity of anatase TiO <sub>2</sub> . International Journal of Modern Physics B, 2017, 31, 1750036.	1.0	3
49	The rule of N in N-doped graphene supported Pd catalyst. Chemical Physics Letters, 2021, 763, 138155.	1.2	3
50	DFT study of N,S co-doped graphene anodes for Na-ion storage and diffusion. New Journal of Chemistry, 2022, 46, 13866-13873.	1.4	3
51	First-principles study of native defects in bulk Sm2CuO4 and its (001) surface structure. Journal of Applied Physics, 2018, 123, .	1.1	2
52	Well dispersed SnO2 nanoclusters preparation and modulation of metal-insulator transition induced by ionic liquid. Chinese Journal of Chemical Physics, 2019, 32, 248-252.	0.6	1
53	CO Adsorption and Oxidation on Metal-Doped TiO <sub>2</sub> Nanotube Arrays. Wuli Huaxue Xuebao/ Acta Physico - Chimica Sinica, 2012, 28, 44-50.	2.2	1

54 Molecular Modeling: Modeling Interactions between Liposomes and Hydrophobic Nanosheets (Small) Tj ETQq0 0 0 ggBT /Overlock 10 Tf